

Supporting Information

Tautomerism and Self-Association in the Solution of New Pinene-Bipyridine and Pinene-Phenanthroline Derivatives

Atena B. Solea ^{1,2}, Ivan Cornu ¹, Vera Deneva ³, Aurelien Crochet ¹, Katharina M. Fromm ², Liudmil Antonov ³, Christophe Allemann ¹ and Olimpia Mamula ^{1,*}

¹ Haute Ecole d'Ingénierie et d'Architecture Fribourg, HES-SO University of Applied Sciences of Western Switzerland, Pérolles 80, CH-1705 Fribourg, Switzerland; Atena-Bianca.Solea@hefr.ch (A.B.S.); ivan.cornu@master.hes-so.ch (I.C.); aurelien.crochet@unifr.ch (A.C.); Christophe.Allemann@hefr.ch (C.A.)

² Department of Chemistry, University of Fribourg, Chemin du Musée 9, CH-1700 Fribourg, Switzerland; katharina.fromm@unifr.ch (K.M.F.)

³ Bulgarian Academy of Sciences, Institute of Organic Chemistry with Centre of Phytochemistry, Acad. G. Bonchev street, bl. 9, 1113 Sofia, Bulgaria; vdeneva@orgchm.bas.bg (V.D.); Lantonov@orgchm.bas.bg (L.A.)

* Correspondence: olimpia.mamulasteiner@hefr.ch

Contents

¹ H-NMR, ¹³ C-NMR Spectra	6
Mass spectra	14
Crystallographic data for 6	Error! Bookmark not defined.

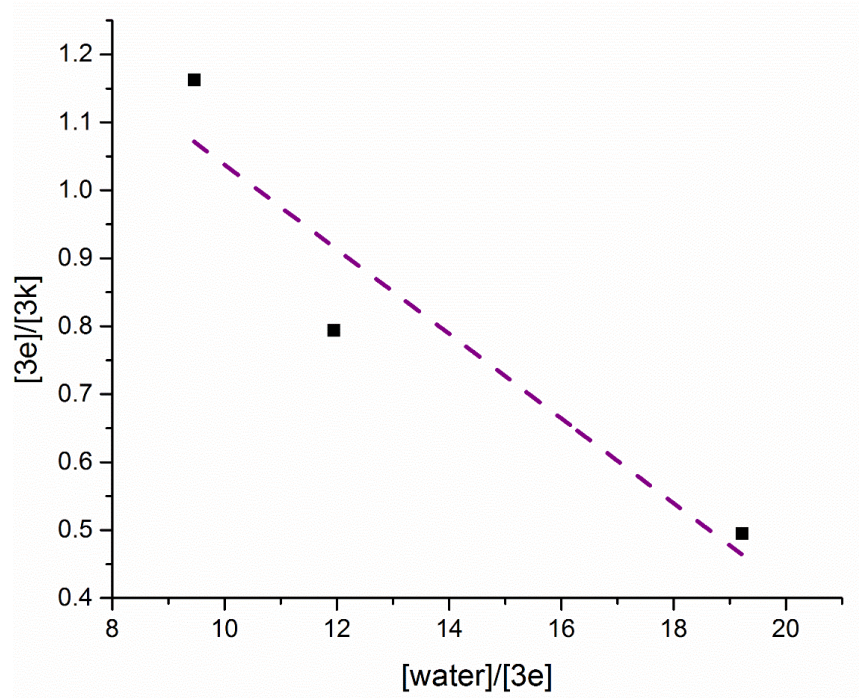


Figure S1. Influence of the water content on the keto-enol equilibrium $3\mathbf{k} \rightleftharpoons 3\mathbf{e}$ (62 mM in CD_3CN)

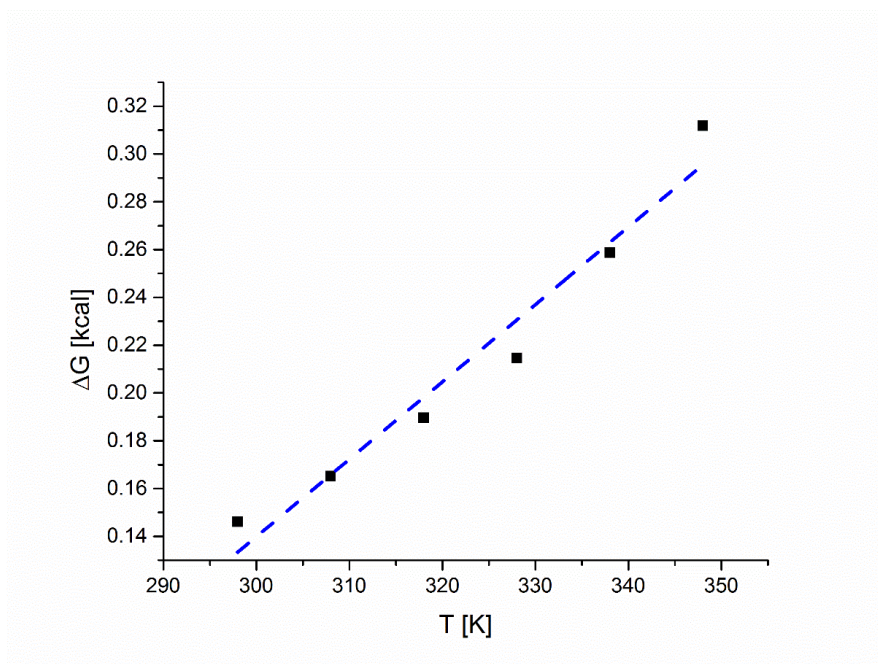


Figure S2. Dependence of the free enthalpy (ΔG°) as a function of temperature for compound 3 (62 mM in CD_3CN), from VT ^1H -NMR experiments

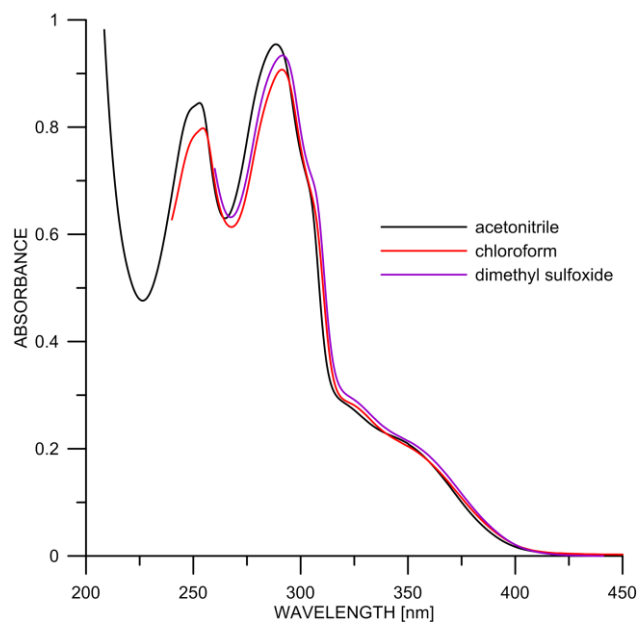
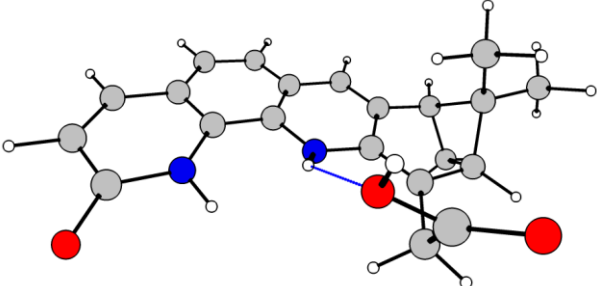
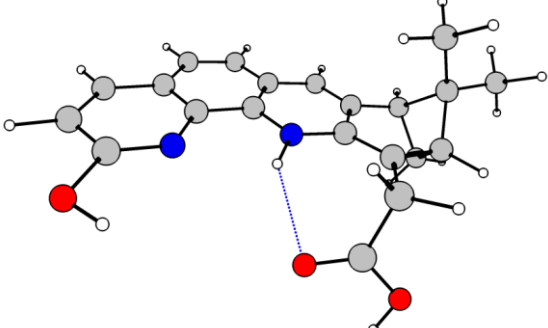
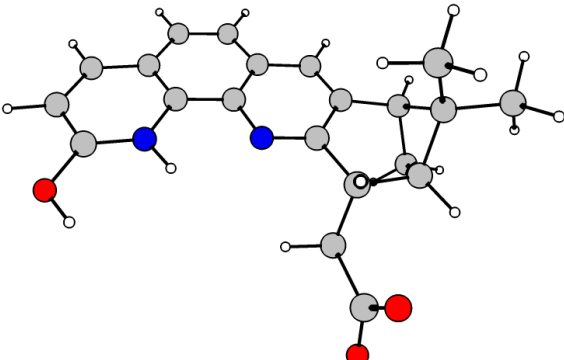
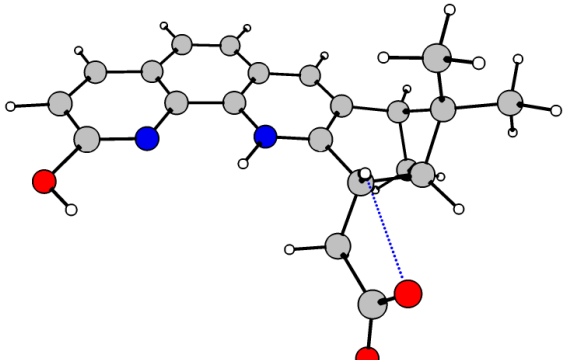


Figure S3. Absorption spectra of **3** in organic solvents.

Table S1. Most stable isomers of the existing tautomers of **6** in chloroform.

Tautomer	ΔE , kcal/mol	μ , D
	0	9.6
	3.0	10.0

	21.4	6.1
	21.1	2.1
	35.4	29.2
	25.3	24.8

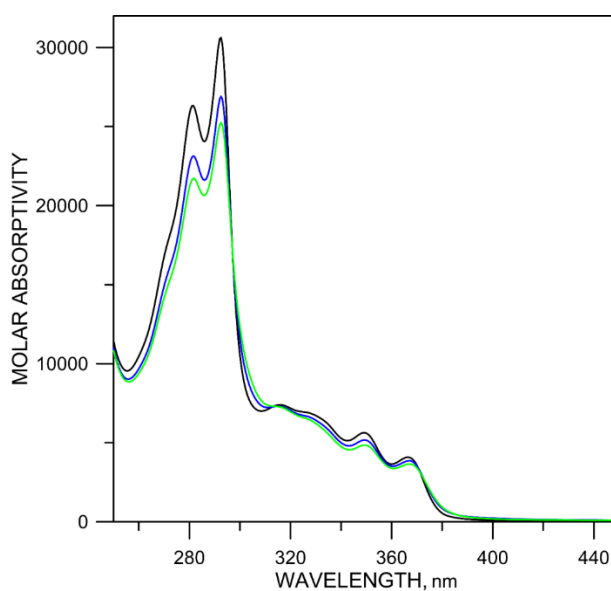
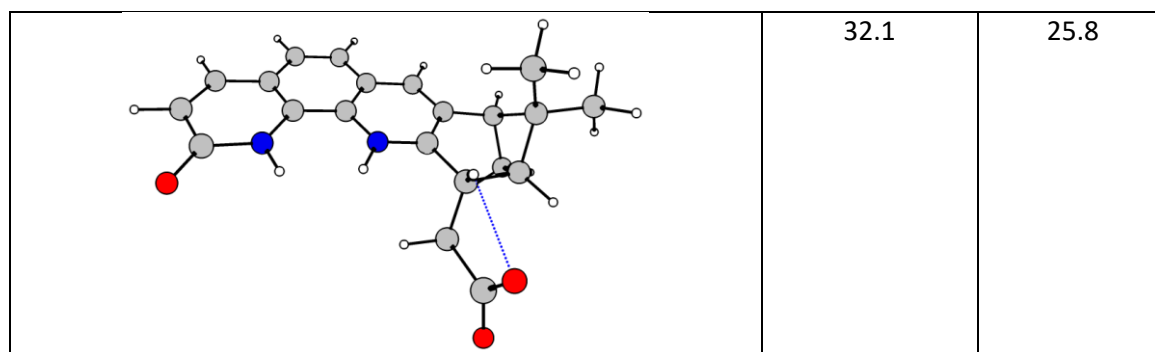


Figure S4. Absorption spectra of **6** in CH_3CN as a function of the concentration while keeping the product between the concentration value and the path length constant ($5.0 \times 10^{-5}\text{M}$). The concentrations are as follows - black solid line: 1.0×10^{-4} M (most concentrated); blue solid line: 5.0×10^{-5} M and green solid line: 5.0×10^{-6} M (most diluted). At concentration higher than 1.0×10^{-4} M no changes are observed.

Table S2. Predicted absorption spectra of the monomer and dimer of **6** in DMSO.

<i>form</i>	<i>B3LYP/6-311+G(2d,p)// M06-2X/TZVP</i>	
	λ_{max} , nm	f^*
<i>monomer</i>	344	0.086
	321	0.037
<i>dimer</i>	343	0.092
	336	0.092
	323	0.010
	321	0.023

* Oscillator strength.

$^1\text{H-NMR}$, $^{13}\text{C-NMR}$ Spectra

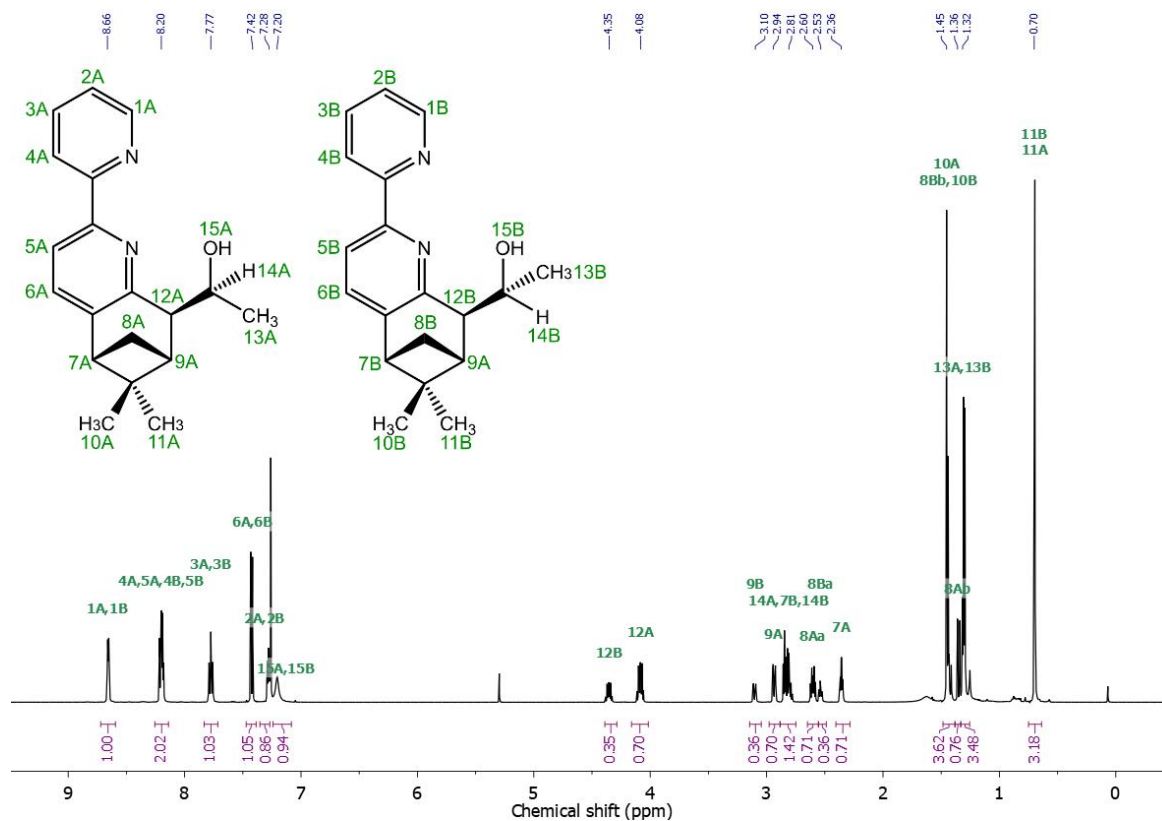


Figure S5. $^1\text{H-NMR}$ spectrum of **2** in CDCl_3 and proton numbering

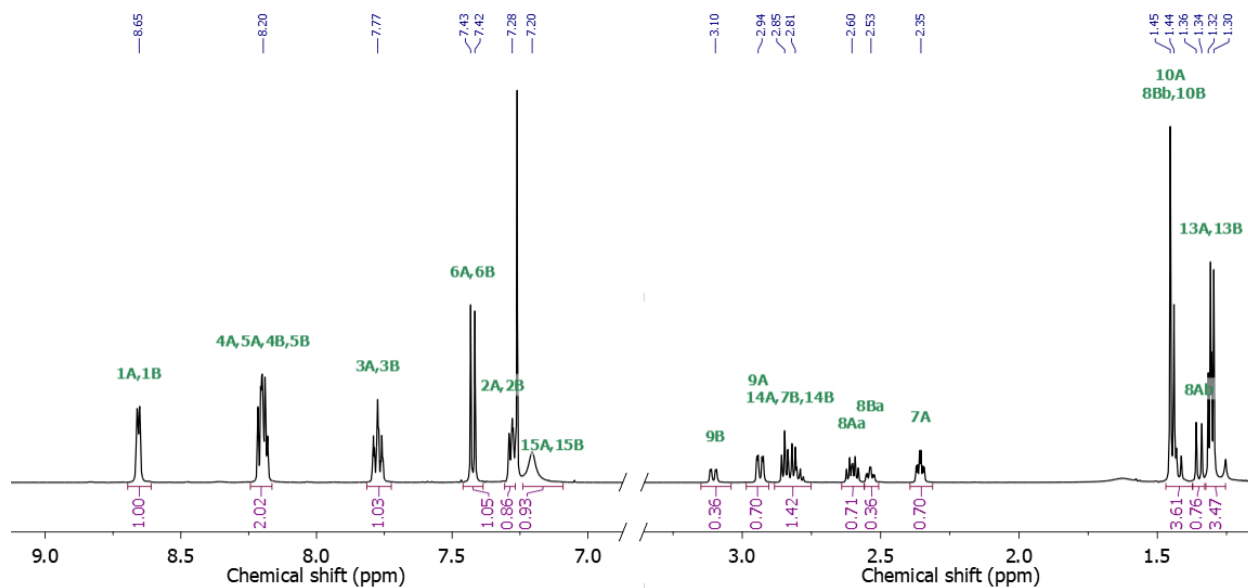


Figure S6. Zoom on the aromatic (left) and aliphatic (right) region of the $^1\text{H-NMR}$ spectrum of **2** in CDCl_3

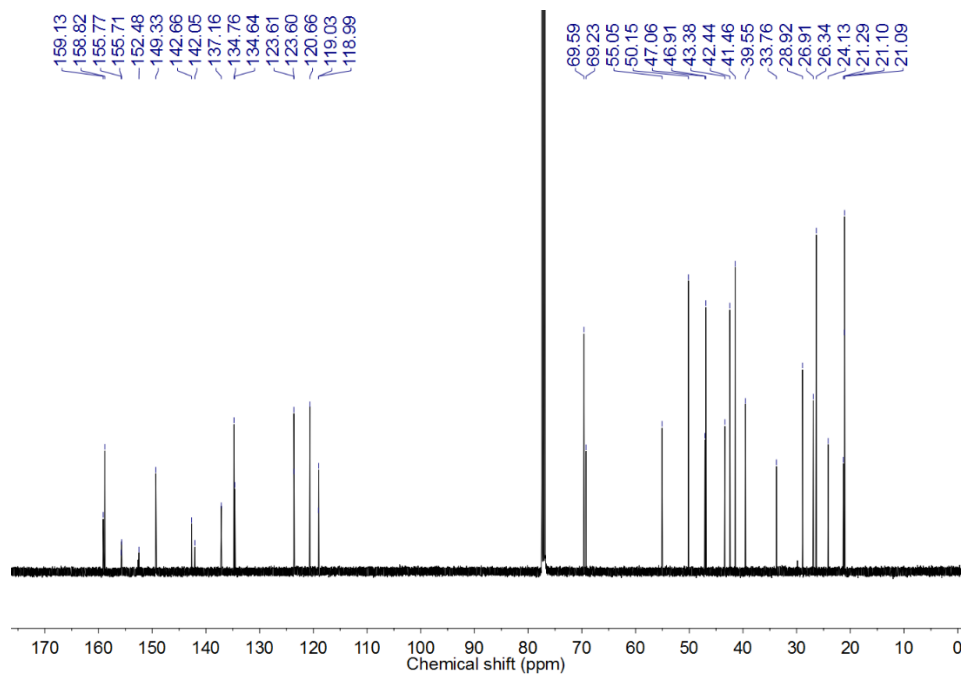


Figure S7. ^{13}C -NMR spectrum of **2** in CDCl_3

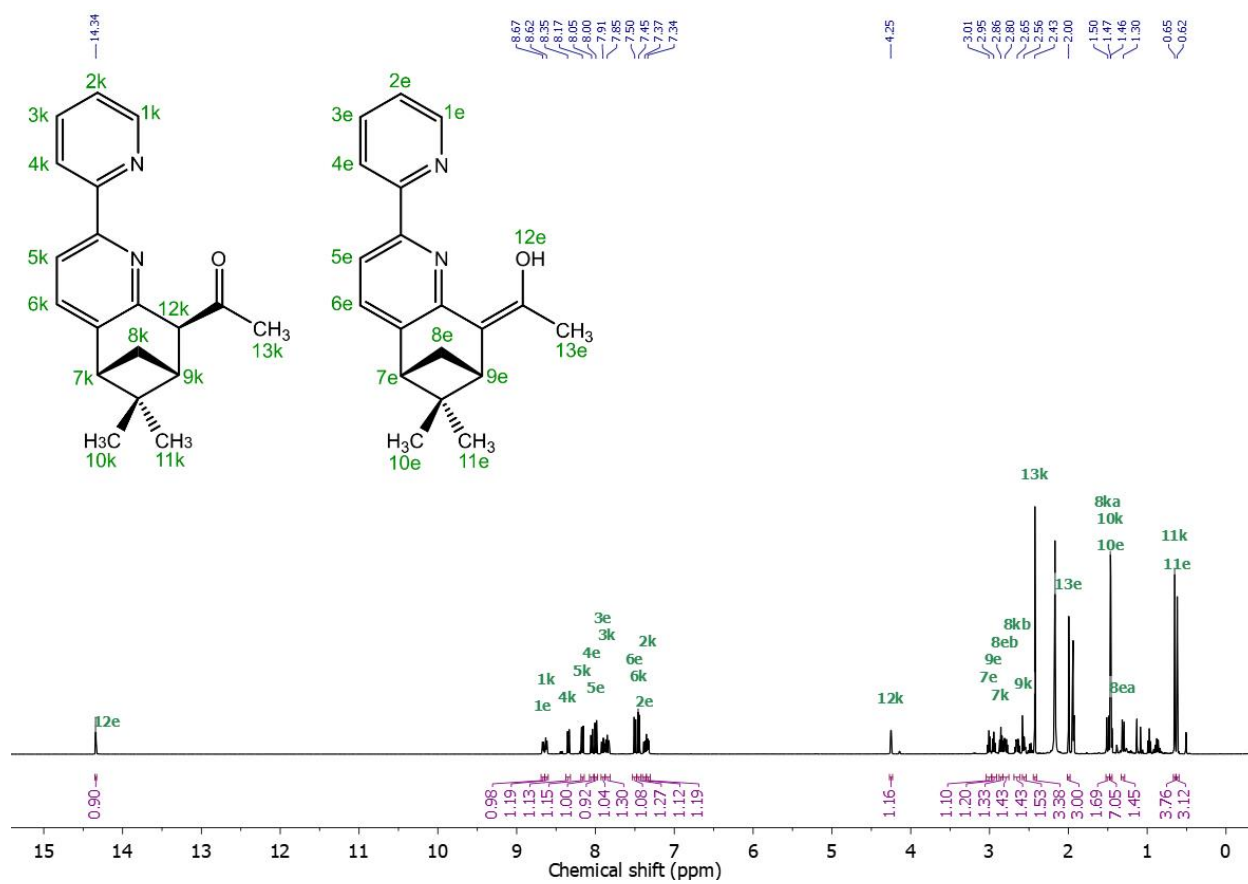


Figure S8. ^1H -NMR spectrum of **3** in CD_3CN and proton numbering

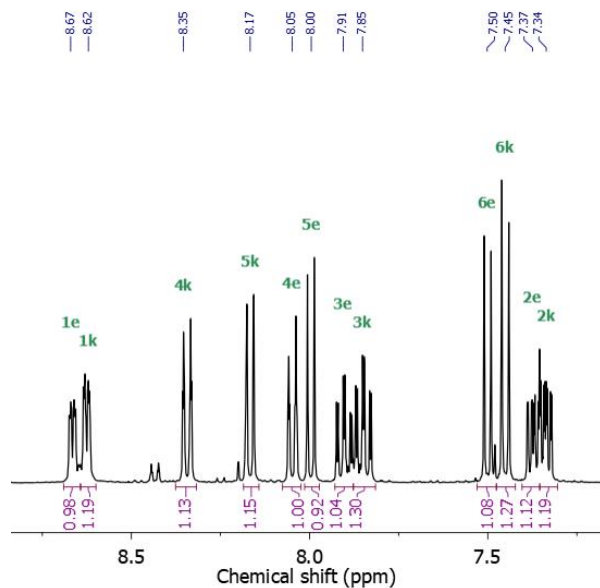


Figure S9. Zoom on the aromatic region of the ^1H -NMR spectrum of **3** in CD_3CN

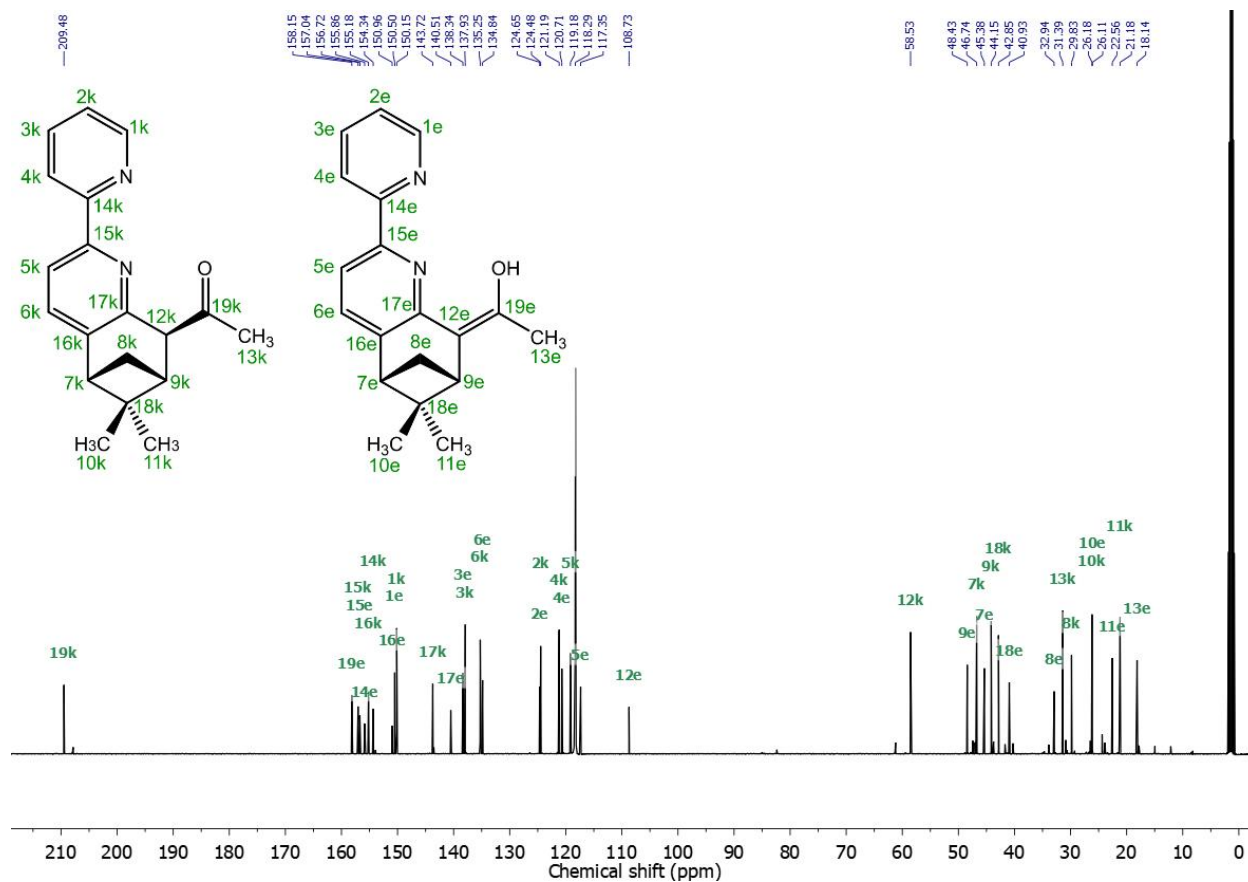


Figure S10. ^{13}C -NMR spectrum of **3** in CD_3CN and carbon numbering

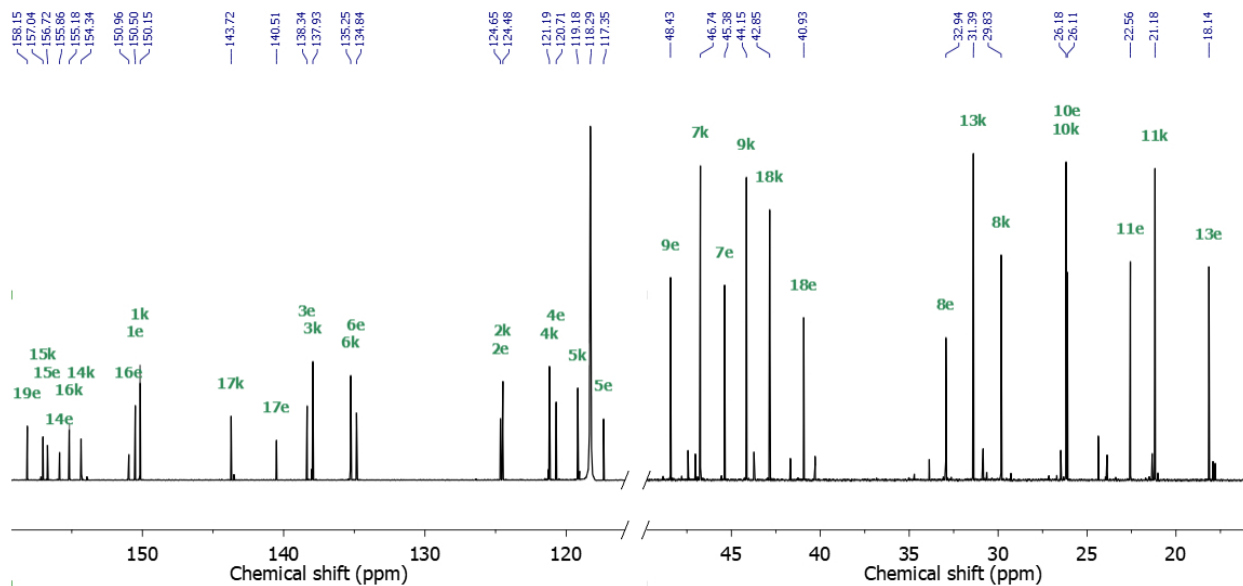


Figure S11. Zoom on the aromatic (left) and aliphatic (right) region of the ^{13}C -NMR spectrum of **3** in CD_3CN

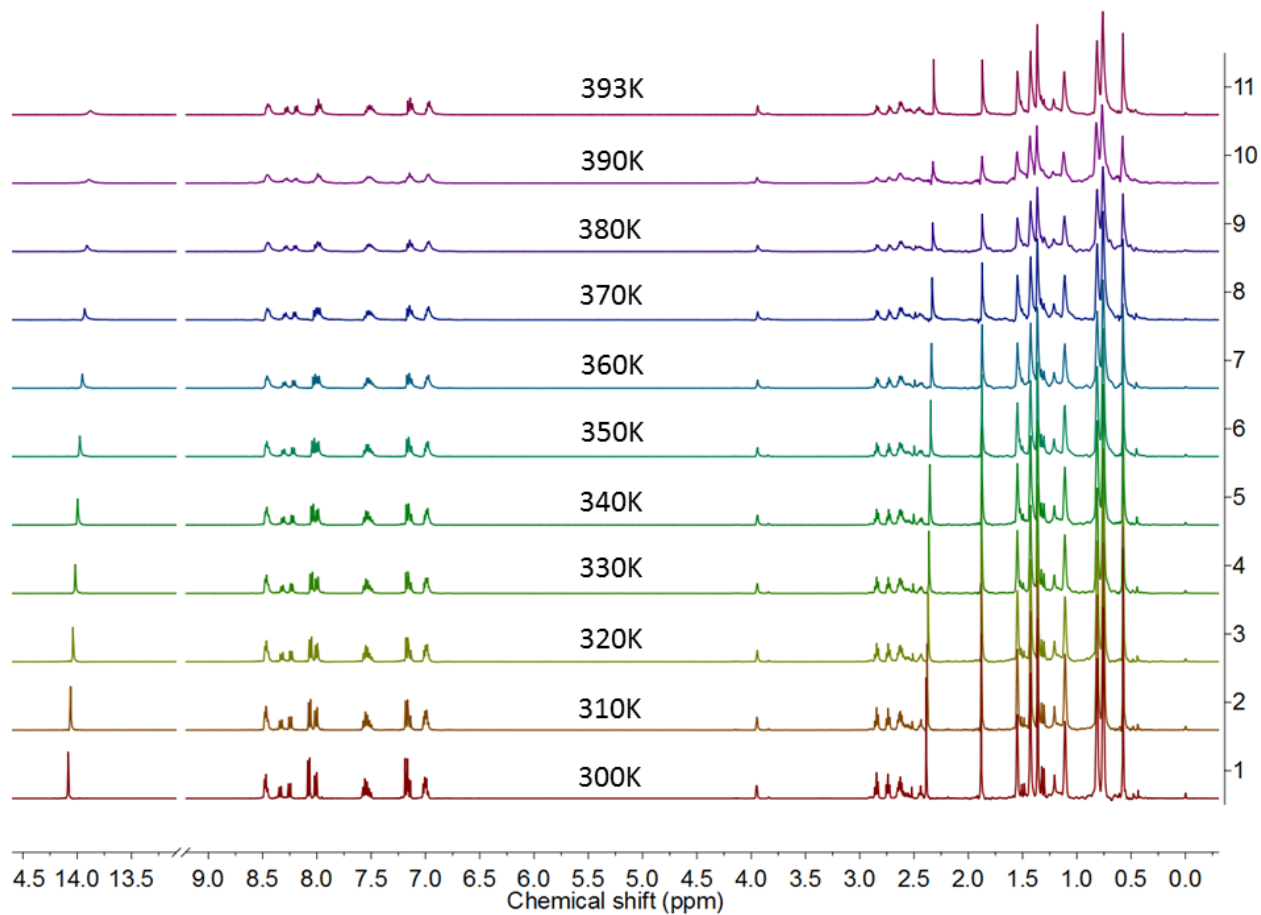


Figure S12. VT- ^1H -NMR spectra of **3** in decalin- d_{18}

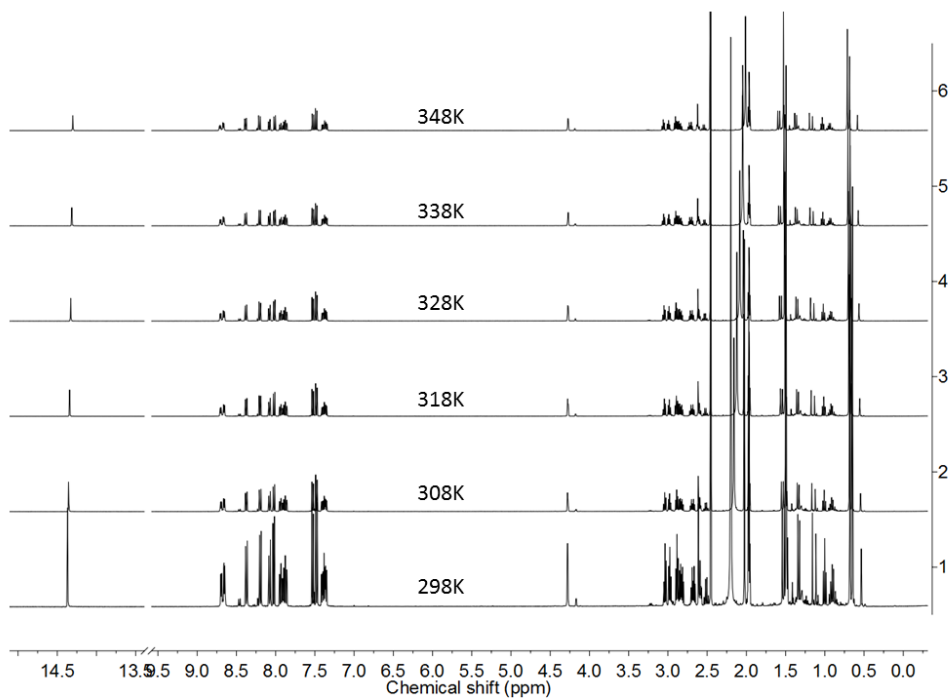


Figure S13. VT- ^1H -NMR spectra of **3** in CD_3CN

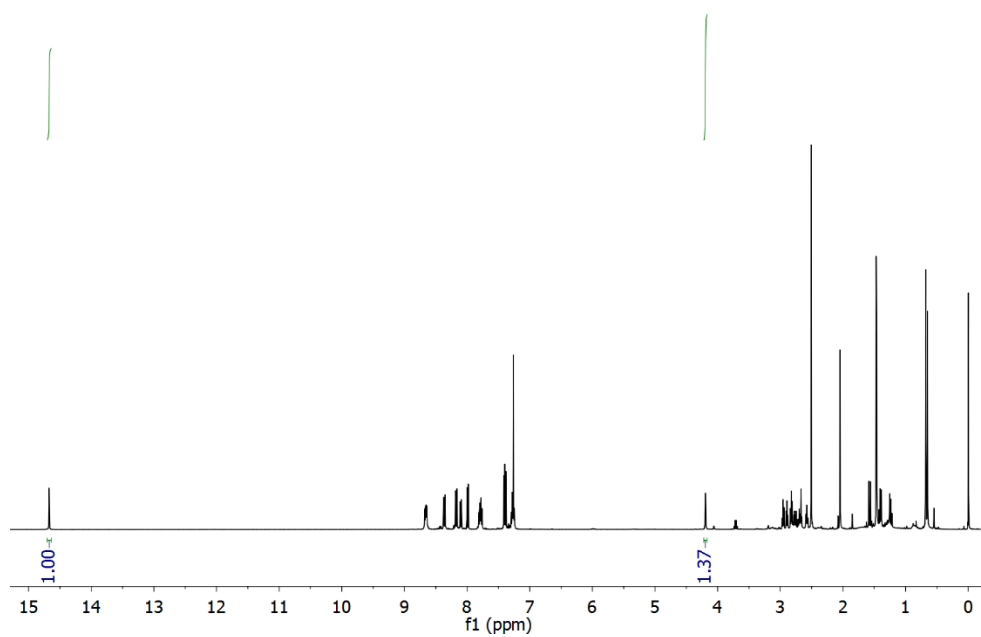


Figure S14a. ^1H -NMR spectrum of **3** in CD_3Cl at 298K

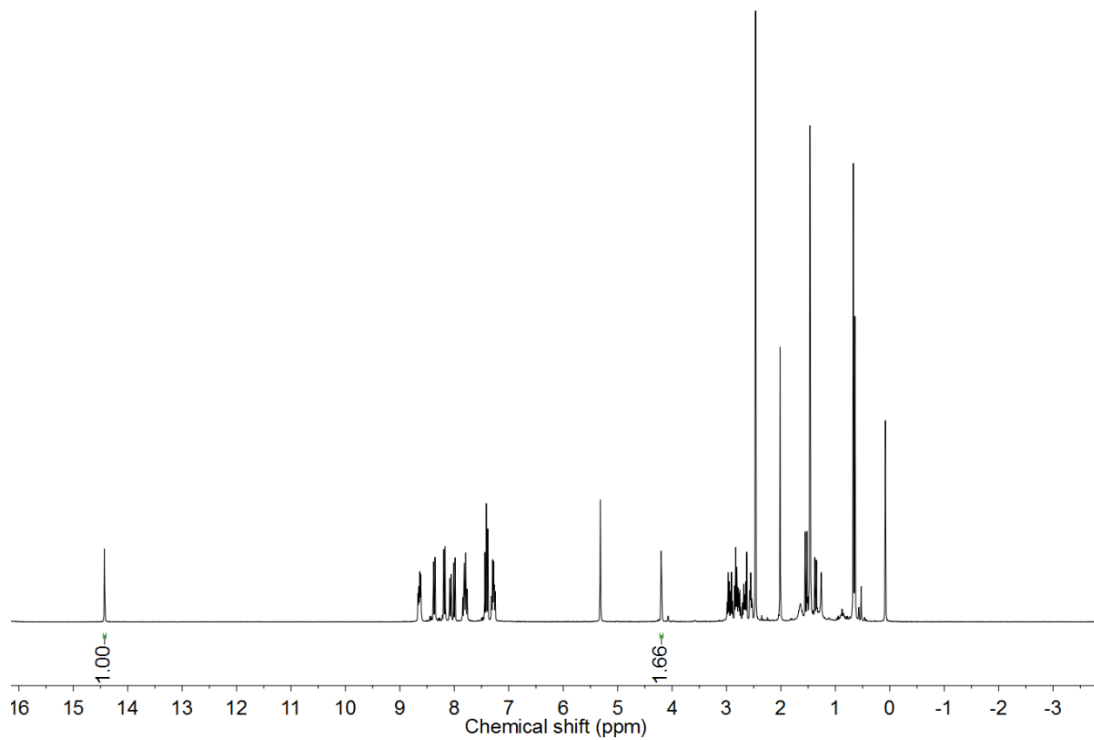


Figure S14b. $^1\text{H-NMR}$ spectrum of **3** in CD_2Cl_2 at 298K

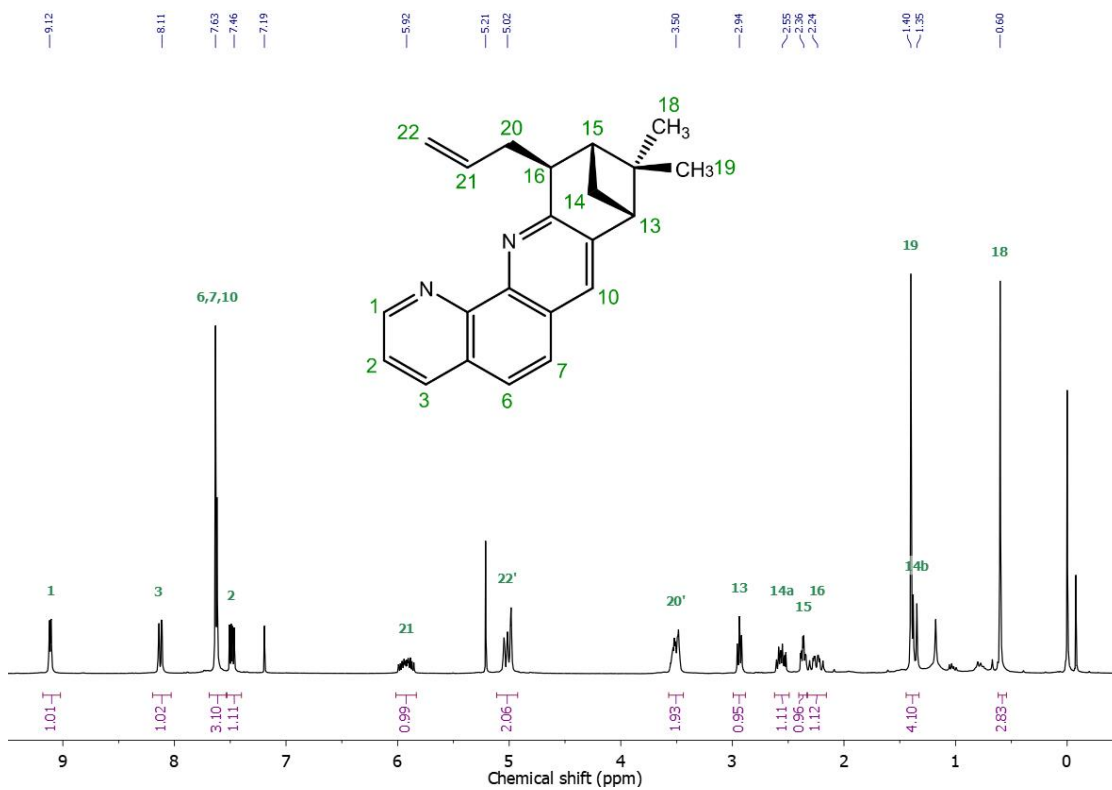


Figure S15. $^1\text{H-NMR}$ spectrum of **5** in CDCl_3 and proton numbering

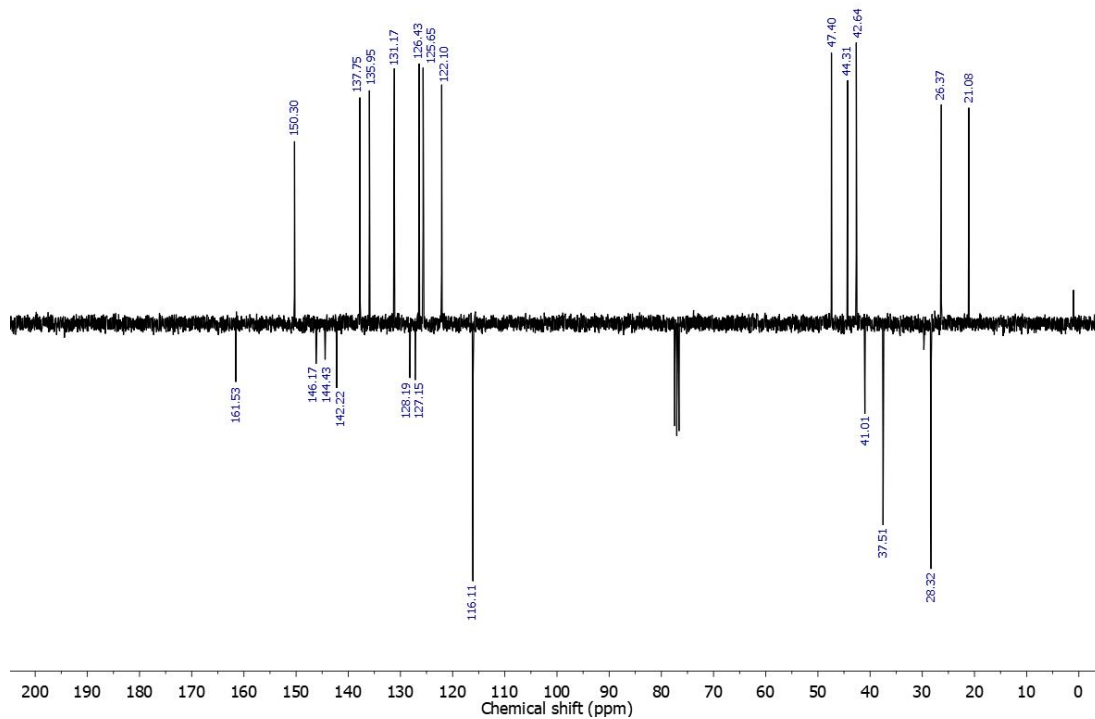


Figure S16. C-APT-NMR spectrum of **5** in CDCl_3

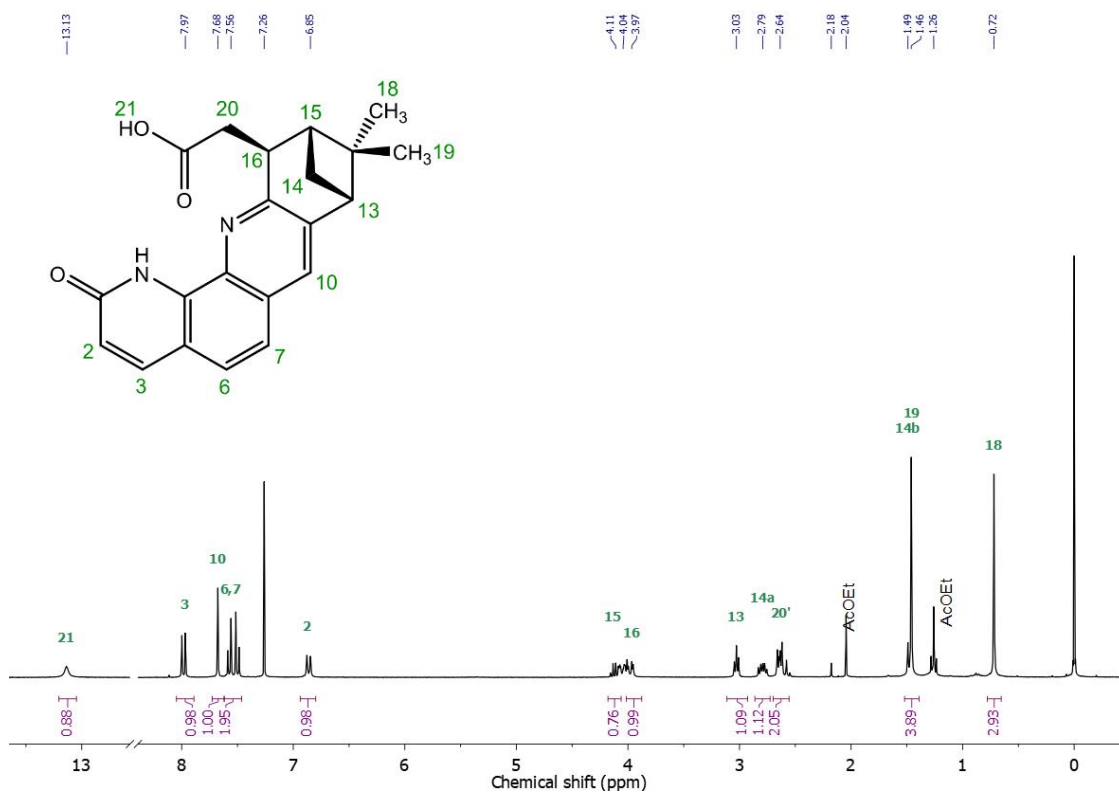


Figure S17. ^1H -NMR spectrum of **6** in CDCl_3 and proton numbering

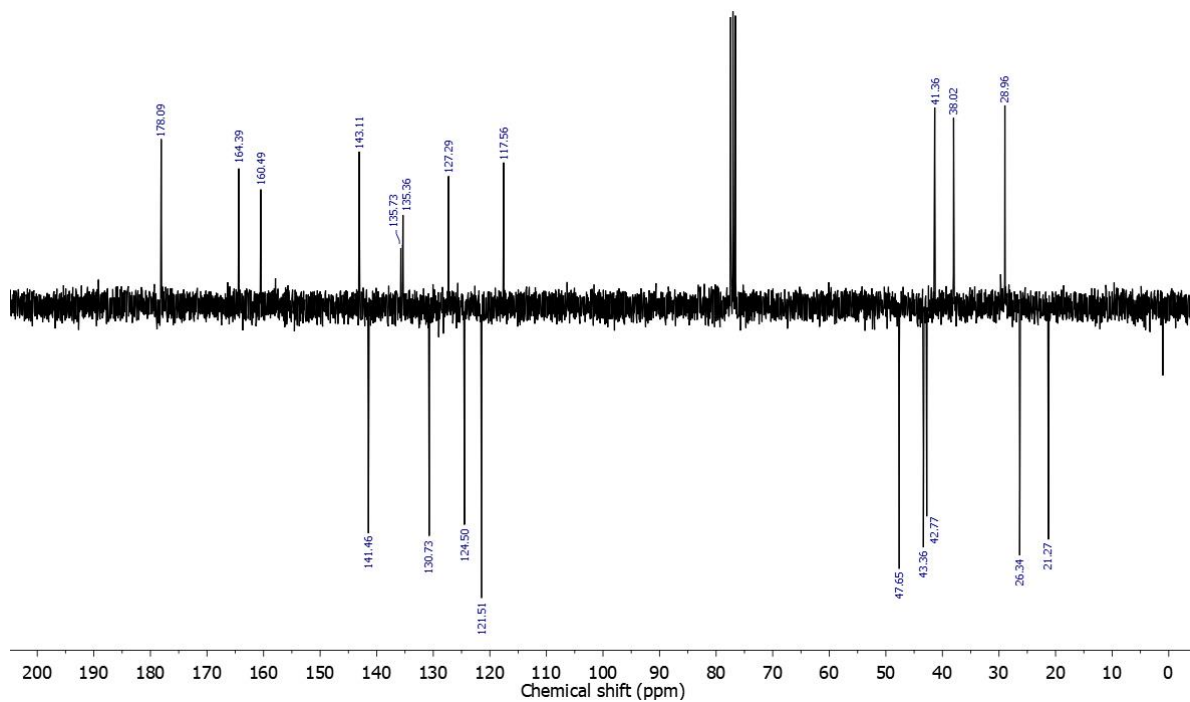


Figure S18. C-APT-NMR spectrum of **6** in CDCl_3

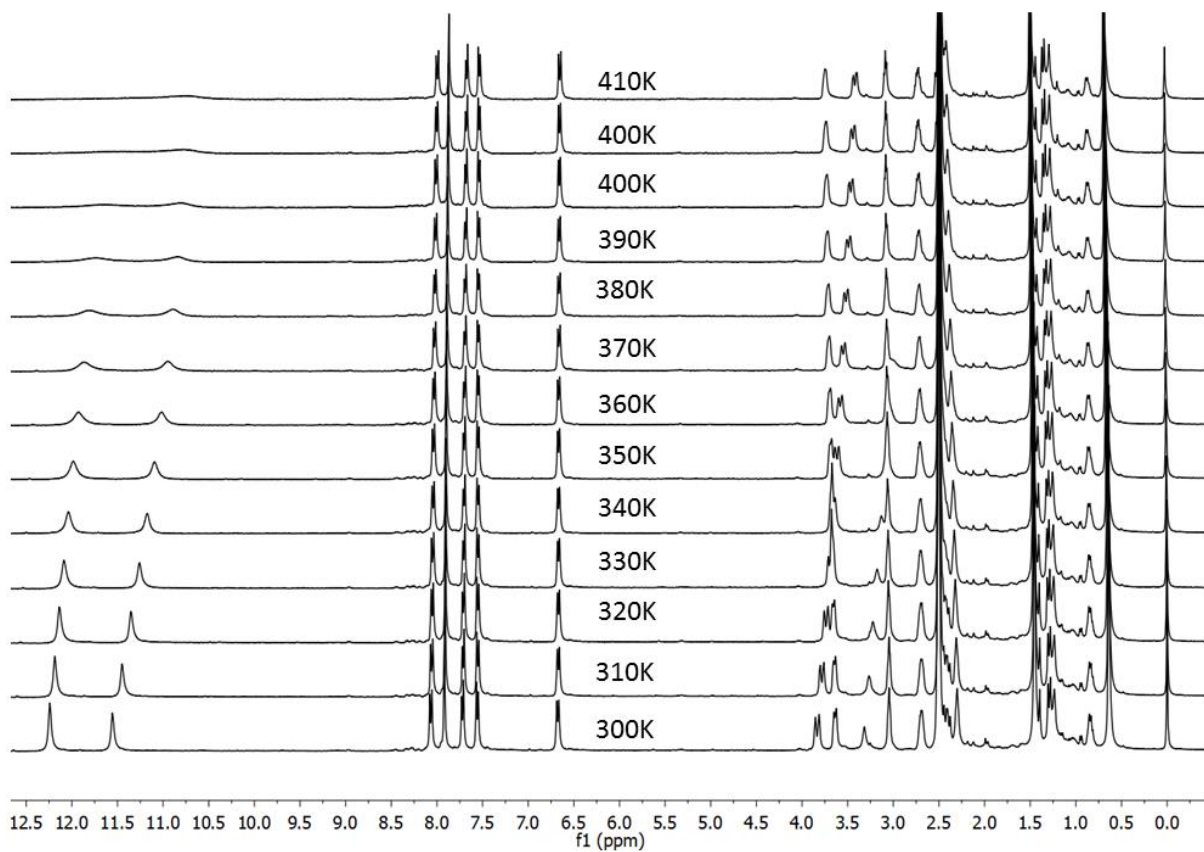


Figure S19. VT-NMR spectra of **6** in DMSO-d_6

Mass spectra

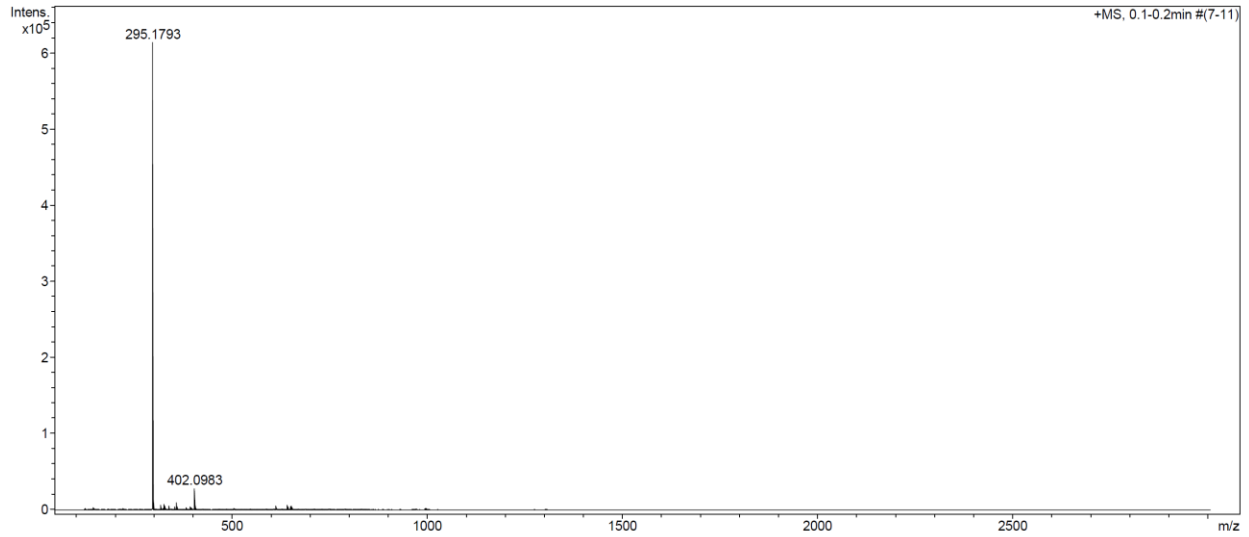
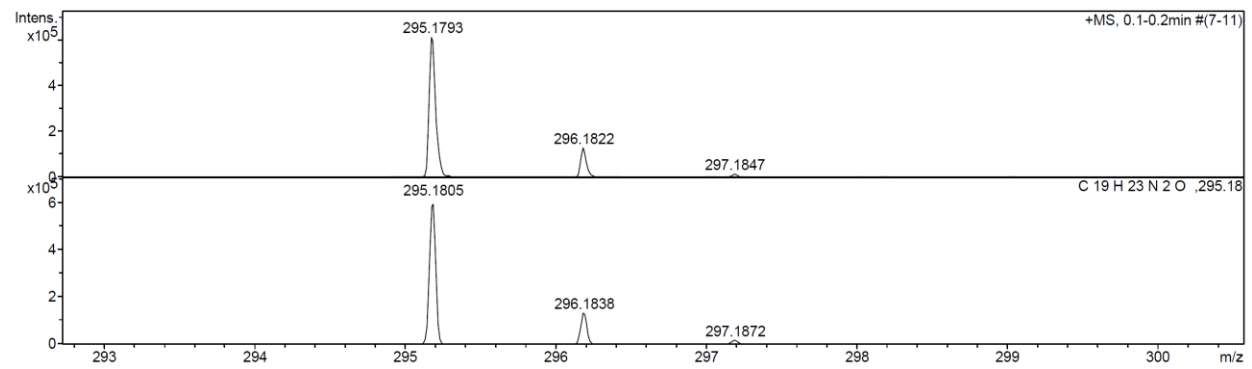


Figure S20. (+)-ESI-MS spectrum of **2**



leas. m/z	#	Formula	m/z	err [ppm]	Mean err [ppm]	rdb	N-Rule	e ⁻ Conf	mSigma	Std I	Std Mean m/z	Std I VarNorm	Std m/z Diff	Std Comb Dev
295.1793	1	C ₁₉ H ₂₃ N ₂ O	295.1805	3.9	4.2	9.5	ok	even	2.50	0.0039	0.0013	0.0016	0.0004	0.8427

Figure S21. HRMS spectrum of **2**

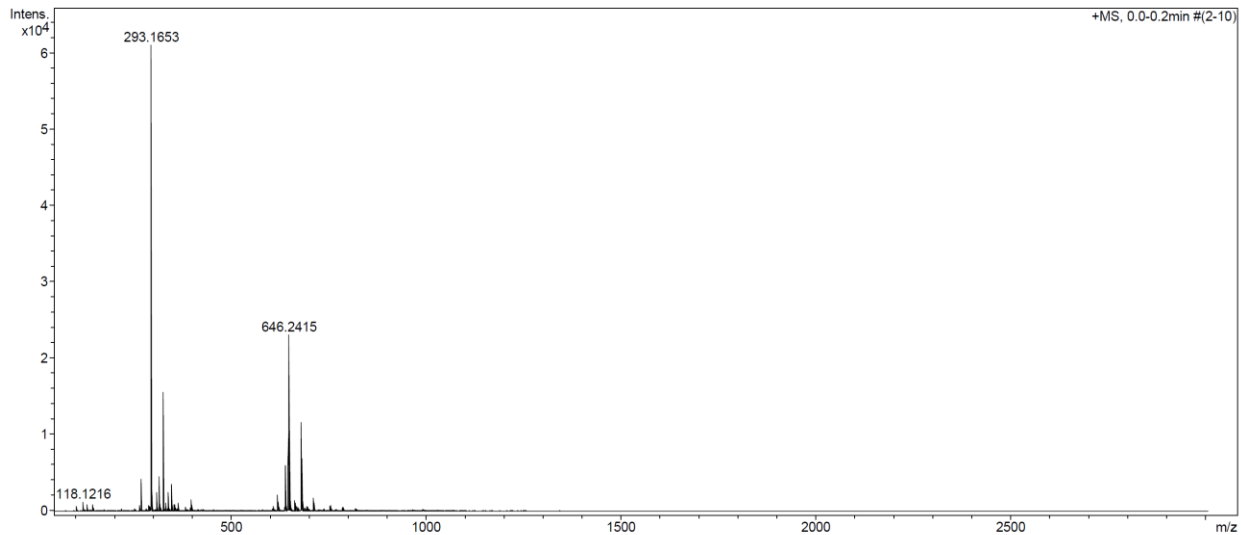
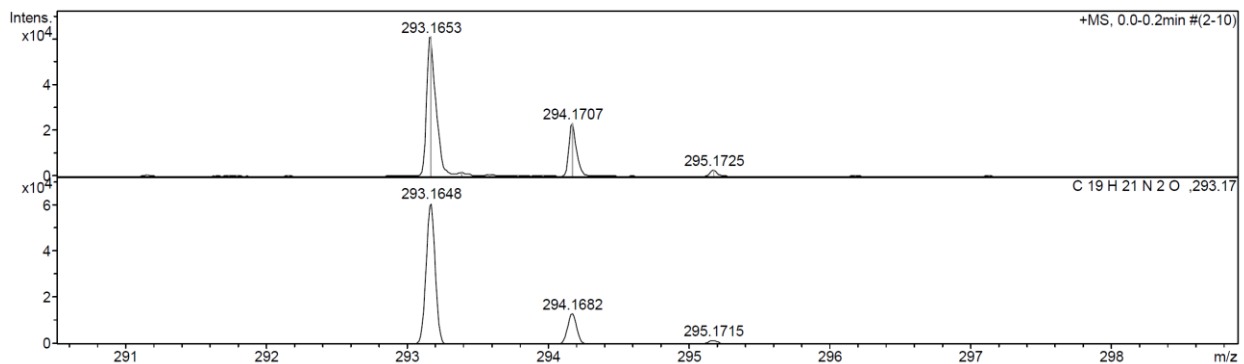


Figure 22. (+)-ESI-MS spectrum of **3**



Obs. m/z	#	Formula	m/z	err [ppm]	Mean err [ppm]	rdb	N-Rule	e ⁻ Conf	mSigma	Std I	Std Mean m/z	Std I VarNorm	Std m/z Diff	Std Comb Dev
293.1653	1	C ₁₉ H ₂₁ N ₂ O	293.1648	-1.4	-3.4	10.5	ok	even	97.29	0.1442	0.0014	0.0569	0.0021	0.8427

Figure S23. HRMS spectrum of **3**

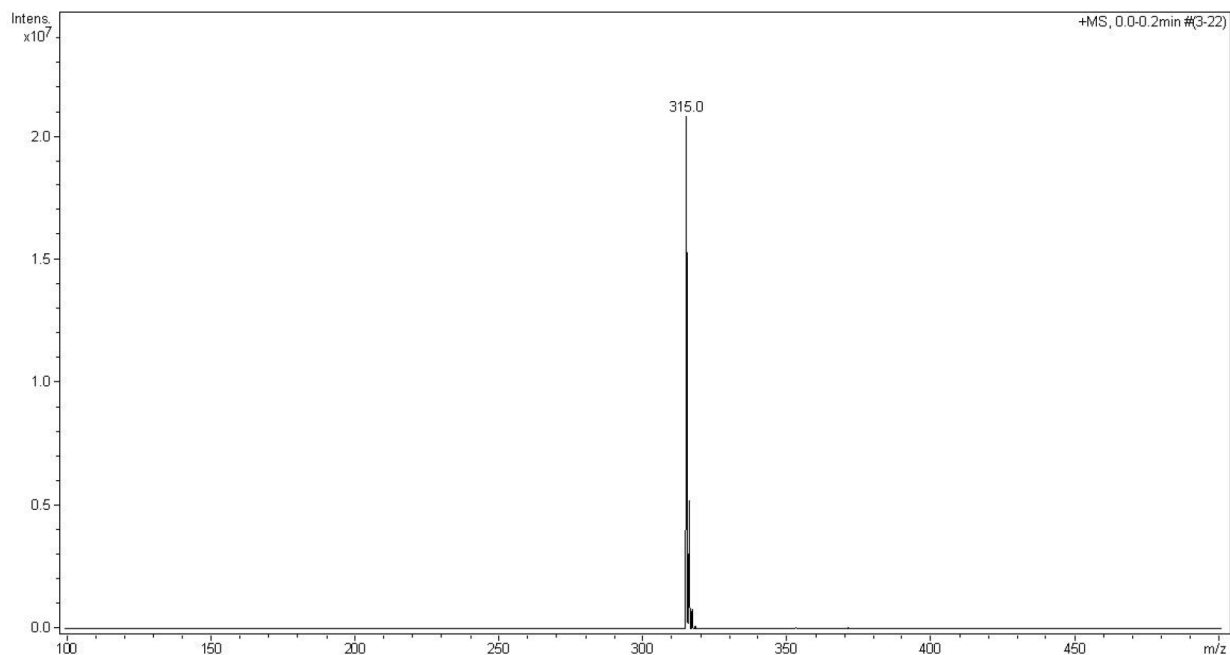


Figure S24. (+)-ESI-MS spectrum of **5**

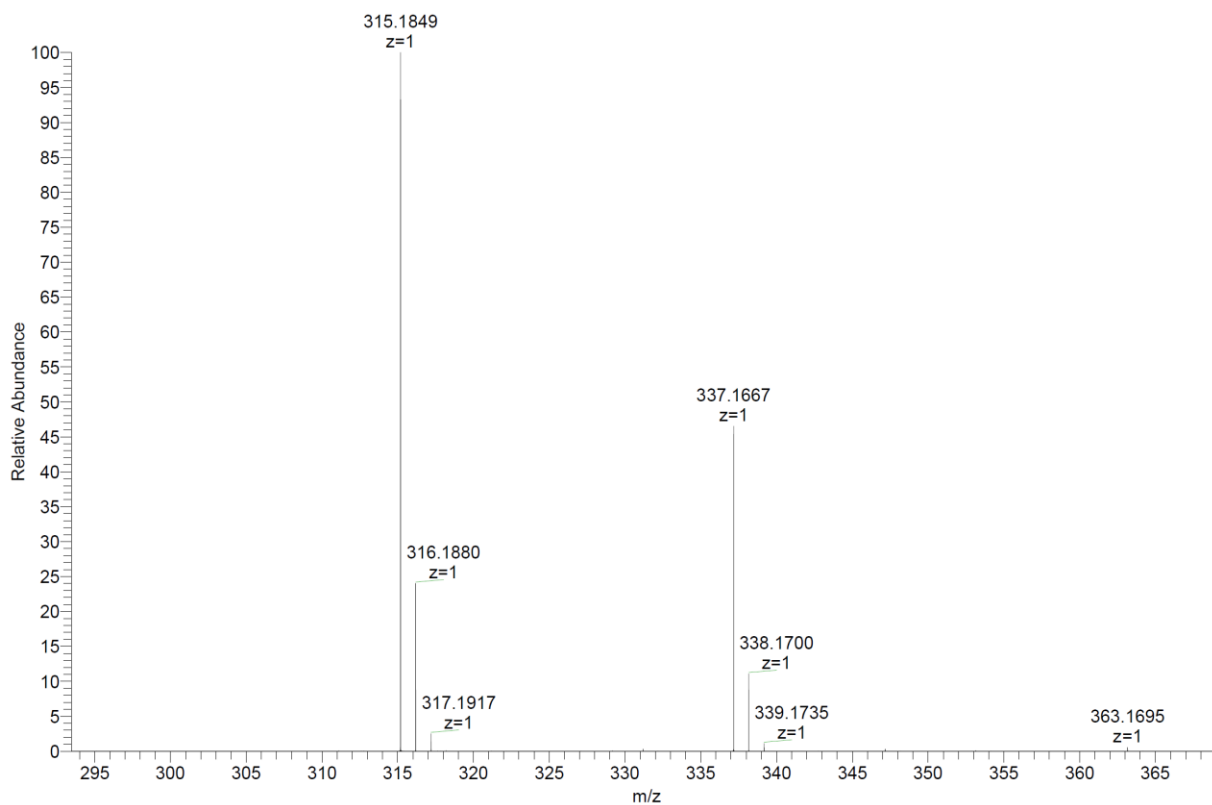


Figure S25. HRMS spectrum of **5**

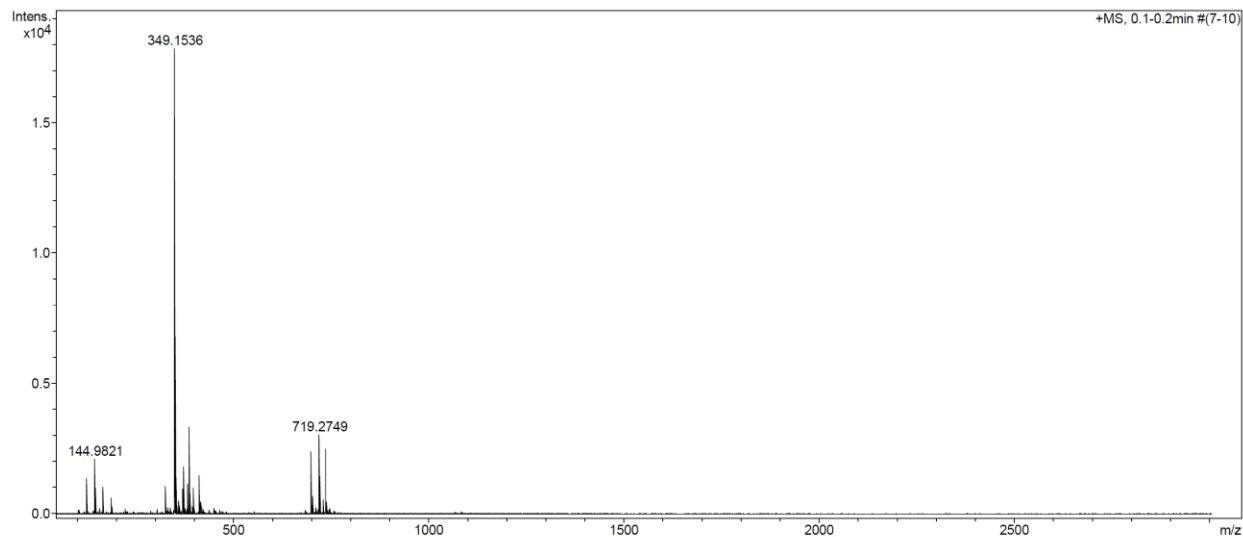
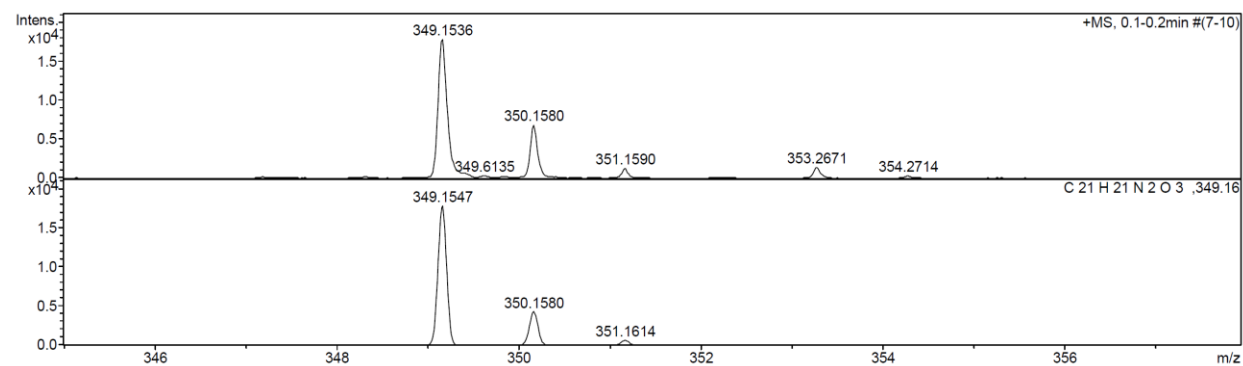


Figure S26. (+)-ESI-MS spectrum of **6**



eas. m/z	#	Formula	m/z	err [ppm]	Mean err [ppm]	rdb	N-Rule	e ⁻ Conf	mSigma	Std I	Std Mean m/z	Std I VarNorm	Std m/z Diff	Std Comb Dev
349.1536	1	C ₂₁ H ₂₁ N ₂ O ₃	349.1547	3.1	2.4	12.5	ok	even	87.77	0.1295	0.0010	0.0546	0.0011	0.8427

Figure S27. HRMS spectrum of **6**

Table S3. Crystallographic data for **6**

Compound	6
CCDC number	1958303
Formula	C ₂₁ H ₂₀ N ₂ O ₃
$D_{calc.}/g\text{ cm}^{-3}$	1.324
μ/mm^{-1}	0.089
Formula Weight	348.39
Colour	colourless
Shape	needle
Size/mm ³	0.32×0.14×0.02
T/K	250(2)
Crystal System	orthorhombic
Space Group	$P2_12_12_1$
$a/\text{Å}$	6.2818(8)
$b/\text{Å}$	14.5974(17)
$c/\text{Å}$	19.054(3)
$V/\text{Å}^3$	1747.2(4)
Z	4
Z'	1
Wavelength/Å	0.71073
Radiation type	MoK α
$\theta_{min} - \theta_{max}/^\circ$	1.757 - 26.365
Measured Refl.	25010
Independent Refl. / restraints/parameters	3517 / 36 / 239
Reflections with $I > 2(I)$	878
R_{int}	0.2809
Largest Peak / Hole / e Å ⁻³	0.141 / -0.173
Deepest Hole	-0.173
Goof	0.675
$R_1, wR_2 (I \geq 2\sigma(I))$	0.2324, 0.0936
R_1, wR_2	0.0462, 0.0625